Applied Ocean Research 26 (2004) 183–197

Applied Ocean Research

www.elsevier.com/locate/apor

# Bottom friction and bedload sediment transport caused by boundary layer streaming beneath random waves

Dag Myrhaug[a,*], Lars Erik Holmedal[a], Håvard Rue[b]

[a]Department of Marine Technology, Norwegian University of Science and Technology, NO-7491 Trondheim, Norway
[b]Department of Mathematical Sciences, Norwegian University of Science and Technology, NO-7491 Trondheim, Norway

Received 26 May 2004; revised 8 March 2005; accepted 24 May 2005

**Abstract**

The effect of boundary layer streaming on sea bed shear stresses, as well as on the mean bedload sediment transport rate, beneath random waves, is investigated. Formulas for the bottom friction and bedload sediment transport under regular waves have been applied to obtain the mean bedload sediment transport rate caused by steady streaming under linear random waves. Friction factors for steady streaming under random waves are also provided. The effect of streaming and second order wave asymmetry on the mean bedload sediment transport rate is discussed.


*Keywords:* Random waves; Streaming; Nonlinear waves; Bottom friction; Bedload transport rate; Stochastic approach

## 1. Introduction

Steady streaming under sinusoidal waves is caused by non-uniformity of the wave boundary layer resulting from spatial variation of the orbital velocities. Vertical velocities generated within the bottom boundary layer under progressive waves are not exactly out of phase with the horizontal velocities, leading to a non-zero time-averaged bed shear stress. The steady streaming for a laminar wave boundary layer was determined by Longuet-Higgins [1]. Based on this work, the streaming-related time-averaged bed shear stress can be expressed in terms of the wave friction factor and the wave number (see, e.g. [2]). Recently Nielsen and Callaghan [3] included the effect of streaming predicting the shear stress and the total sediment transport rate for sheet flow under waves. The effect of streaming was included by adding a constant shear stress corresponding to the streaming-related bed shear stress and by applying a friction factor for rough turbulent flow. This method predicts the real propagating wave observations of Ribberink et al. [4] quite well.

A summary of results from models and experiments on wave-induced streaming near the seabed is given by Davies and Villaret [5–7]. Above a smooth bed, the measured streaming at the edge of the wave boundary layer is in reasonable agreement with the Eulerian drift predicted by Longuet-Higgins [1]. Over a flat rough bed, however, the Eulerian drift is reduced in magnitude. The reason is that the phase difference between the outer velocity and the near-bed velocity is smaller for rough turbulent flow than for laminar flow. This feature is described by Trowbridge and Madsen [8] for flows in which momentum transfer is dominated by turbulent processes, i.e. for $A/z_0 \gtrsim 900$, where $A$ is the near-bed orbital displacement amplitude and $z_0$ is the bed roughness. Trowbridge and Madsen [8] also included the effect of second order wave asymmetry by including second order terms in a specified time-varying eddy viscosity for flow over flat rough beds. They found that this reduced the Eulerian drift at the edge of the boundary layer with a mean flow reversal (negative drift) occurring for very long waves, i.e. for small $kh$, where $k$ is the wave number and $h$ is the water depth. Davies and Villaret [7] have developed an analytical model of the Eulerian drift induced by second order Stokes waves in the wave boundary layer above very rough and rippled beds. They found that the streaming velocity profile within the wave boundary layer is characterized by: a near-bed jet in the direction of

* Corresponding author. Tel.: +47 73 59 5527; fax: +47 73 59 5697.
*E-mail address:* dagmyr@marin.ntnu.no (D. Myrhaug).

0141-1187/$ - see front matter 
doi:10.1016/j.apor.2005.05.001

wave propagation; a level of zero velocity; and a flow reversal extending to the edge of the boundary layer. The negative streaming velocity at the edge of the boundary layer depends on the wave height to water depth ratio, the degree of wave asymmetry, and the near-bed displacement amplitude to bed roughness ratio. For very rough and rippled beds the momentum transfer is no longer dominated by turbulent processes but by organized vortices shed from bed roughness elements or ripple crests at flow reversal. As a result, they found that the drift at the edge of the wave boundary layer was in the negative wave direction. More details are given in Davies and Villaret [7].

The purpose of this paper is twofold. First, to investigate the effect of streaming on the bed shear stresses beneath random waves and to compare the magnitude of these streaming-related bed shear stresses with those for linear waves. Second, to investigate the effect of streaming on the bedload sediment transport rate beneath random waves and to compare the magnitude of this effect with that caused by second order asymmetric waves as determined by Myrhaug and Holmedal [9]. The asymmetric wave motion gives a non-zero net sediment transport in the direction of wave propagation, because transport under the crest is greater than under the trough. The present results are valid for flows over flat rough beds with $A/z_0 \gtrsim 900$, for which the momentum transfer is dominated by turbulent processes. The present analysis of bed shear stresses has physical implications for the estimation of wave energy dissipation for flow above rough beds. The results for the bedload transport rate is particularly relevant to shingle and coarse sand, where all or at least most of the sediment transport takes place as bedload. The *rms* (root-mean-square) friction factors and the mean bedload transport rate for random waves are provided.

The reader should note the difference between the two effects considered here; the second order wave asymmetry and streaming. By the second order wave asymmetry effect is meant that the magnitude of the wave crest velocity is larger than that of the wave trough velocity at the edge of the boundary layer, inducing a net drift in the wave propagation direction. Streaming is caused by the presence of a vertical velocity component in the boundary layer under progressive waves giving a weak current at the edge of the boundary layer. For the parameter regime considered here, this current is in the wave propagation direction.

Previous studies of bottom friction beneath random waves have been undertaken by Madsen, Simons et al., Myrhaug, Myrhaug et al., Mathiesen and Madsen, Samad, Holmedal et al. [10–19] as well as Myrhaug and Holmedal [20–22]. Madsen [10] gave explicit wave friction factor formulas for spectral wave-current boundary layer flow. The formulas were obtained using a time-invariant eddy viscosity model based on the concept of an equivalent sinusoidal wave having the same near-bed orbital velocity amplitude and excursion amplitude as the *rms* value of the wave spectrum. Laboratory experiments studying the bed boundary layer under random waves plus currents were carried out by Simons et al. [11,12] and by MacIver and Simons in 1998 (see [14]). All these measurements were performed in the basin at the UK Coastal Research Facility allowing for waves having an angle of attack on the current. Myrhaug [13] showed that if the free surface elevation is assumed to be stationary Gaussian narrow-band process, the bed shear stress maximum for waves alone is Weibull distributed. This approach was successfully compared with estimates of bed shear stresses under random waves from field measurements near the seabed in the Strait of Juan de Fuca, Washington State, and at EDDA, North Sea, in Myrhaug et al. [15]. Myrhaug [13] approach was extended by Myrhaug et al. [14] to weak wave-current interactions. Mathiesen and Madsen[16] investigated the bottom roughness for spectral waves and current. Their experiments show that sinusoidal and spectral wave-current bottom boundary layer flow over a fixed rippled bed can both be characterized by a single bottom roughness when used in conjunction with a representative equivalent wave. Samad [17] investigated laminar and smooth turbulent flow characteristics in the bed boundary layer under irregular waves. He performed systematic experimental investigations as well as computations using a $k-\varepsilon$ model. Shear stress amplitudes under random waves plus current have been calculated by Holmedal et al. [18] using Monte Carlo simulations of Soulsby [23] parameterized wave-current friction factor formulas valid for sinusoidal waves plus current. Holmedal et al. [19] used a dynamic eddy viscosity ($k-\varepsilon$) model to investigate the seabed boundary layer under random waves plus current. Myrhaug and Holmedal [20] extended Myrhaug et al. [14] approach to calculate the bottom friction in nonlinear random waves plus current flow near a rough bed in the lower near-bed excursion amplitude to bed roughness range. Myrhaug and Holmedal [21] used a similar approach to calculate the laminar bottom friction beneath nonlinear random waves. Myrhaug and Holmedal [22] used a similar approach as used in this paper to investigate the effect of boundary layer streaming on the seabed shear stresses, beneath random waves, for laminar flow and smooth turbulent flow.

Previous studies of bedload transport rate under random waves have been undertaken by Myrhaug and Holmedal [9] as well as Holmedal and Myrhaug [24]. The first reference calculated analytically the bedload transport rate under random second order Stokes waves using a simple bedload formula by Damgaard et al. [25] for each individual wave component. The second reference calculated the flat bed bedload transport rate under random waves plus current using Monte Carlo simulations of Soulsby's [23] parameterized wave-current friction factor formulas combined with his bedload transport formula valid for sinusoidal waves plus current.

## 2. Effect of streaming under regular waves

### 2.1. Bottom friction caused by streaming

Following Nielsen [2] the bottom shear stress related to the wave-induced current (streaming) in the laminar bottom boundary layer of regular waves is given as follows:

$$\frac{\tau_{str}}{\rho} = \frac{1}{2\sqrt{2}} k \sqrt{\frac{\nu}{\omega}} U^2 \quad (1)$$

where $U$ is the near-bed orbital velocity amplitude, $\omega$ is the angular wave frequency, $\rho$ is the density of the fluid, $\nu$ is the kinematic viscosity of the fluid, $k$ is the wave number determined from the dispersion relationship $\omega^2 = gk \tanh kh$, $g$ is the acceleration of gravity, and $h$ is the water depth. Eq. (1) can be re-arranged to:

$$\frac{\tau_{str}}{\rho} = \frac{1}{4\sqrt{2}} kA^3\omega^2 f_w = \frac{1}{4\sqrt{2}} kAf_w U^2 \quad (2)$$

where $A = U/\omega$ is the near-bed orbital displacement amplitude and $f_w$ is the laminar wave friction factor given as that for Stokes' second problem ([26]): $f_w = 2\,Re^{-0.5}$ for $Re \lesssim 3.10^5$, where $Re = UA/\nu$ is the Reynolds number associated with the wave motion.

Nielsen and Callaghan [3] have recently applied Eq. (2) for rough turbulent flow to include the effect of streaming in shear stress and sediment transport calculations for sheet flow under waves. They used a modified version of Swart [27] friction factor proposed by [2]. In this paper, rough turbulent flow will be considered using the friction factor proposed by [14] for $A/z_0 \gtrsim 200$

$$f_w = c\left(\frac{A}{z_0}\right)^{-d} \quad (3)$$

with the coefficients

$$(c, d) = (1.39, 0.52) \quad \text{for} \quad 900 \lesssim A/z_0 \lesssim 11000 \quad (4)$$

$$(c, d) = (0.112, 0.25) \quad \text{for} \quad 11000 \lesssim A/z_0 \quad (5)$$

Note that Eq. (4) corresponds to Soulsby [23] friction factor obtained as best fit to data for $10 \lesssim A/z_0 \lesssim 10^5$. The reason for using this friction factor is that it is possible to derive the stochastic approach analytically, which is not possible by using, e.g. the Swart formula. Note that the results which will be deduced here using Eq. (4) will be valid for $A/z_0 \gtrsim 900$.

Application of the friction factor for rough turbulent flow should be considered as a first approximation to the streaming related shear stress for rough turbulent flow. This is encouraged by the success of Nielsen and Callaghan [3] in predicting the total sediment transport rate data of Ribberink et al. [4]. Moreover, the results shown in Fig. 1 give some support for the method. It shows $\tau_{str}/(\rho U^2\, kA)$ versus $A/z_0$ in the range $9.10^2 \le A/z_0 \le 3 \cdot 10^5$, compared with the results of [28]; Fig. 7.2 from a two-equation $(k-\varepsilon)$ turbulence closure model. Overall the results by the two methods are in fair agreement for engineering purposes.

### 2.2. Bedload transport caused by streaming

The bedload transport caused by streaming is calculated using the Soulsby [23], Eqs. SC (129a)–SC(129d) formulas for bedload transport by regular waves plus current. The reason is that the wave motion, with the effect of streaming included, can be modelled by waves plus a weak current caused by streaming. This corresponds to the wave-dominated situation for co-linear waves plus current, which is obtained by using Soulsby [23], Eq. SC(129b)) formula, as

$$\Phi_{str} = \alpha\theta_w^{1/2} \cdot \theta_{str}; \quad \alpha = 13.7 \quad (6)$$

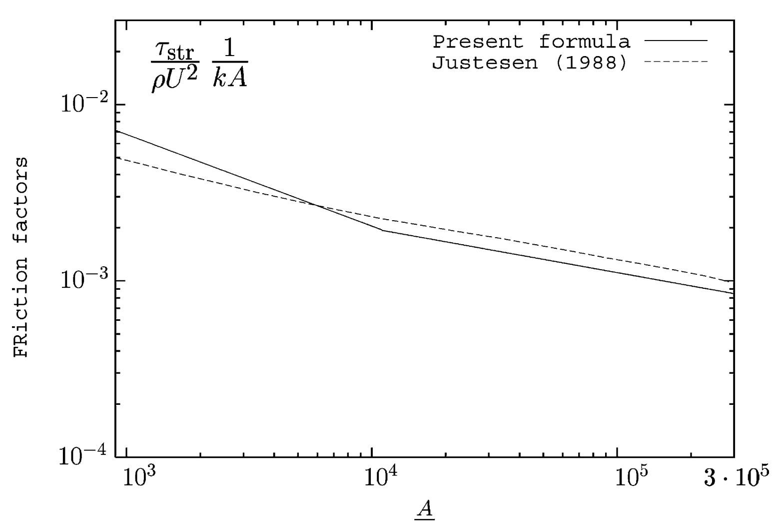


Fig. 1. Friction factor due to streaming vs. $A/z_0$ for sinusoidal waves.

where

$$\Phi_{\rm str} = \frac{q_{\rm bstr}}{[g(s-1)d_{50}^3]^{1/2}} \tag{7}$$

$$\theta_w = \frac{\tau_w}{\rho g(s-1)d_{50}} \tag{8}$$

$$\theta_{\rm str} = \frac{\tau_{\rm str}}{\rho g(s-1)d_{50}} \tag{9}$$

Here $\Phi_{\rm str}$ is the dimensionless bedload transport rate caused by streaming, $\theta_w$ is the amplitude of the oscillatory component of the Shields parameter, $\theta_{\rm str}$ is the Shields parameter caused by streaming, $q_{\rm bstr}$ is the volumetric net bedload transport rate per unit width [m$^2$/s], $s$ is the sediment density to fluid density ratio, and $d_{50}$ is the median grain size diameter. Eq. (6) applies only if $\theta_w$ is larger than the threshold value $\theta_{\rm cr}$ where $\theta_{\rm cr}$ is the critical value of the Shields parameter corresponding to the initiation of motion of the bed, i.e. $\theta_{\rm cr} \approx 0.05$. The expression for $\Phi_{\rm str}$ in Eq. (6) can be viewed as the product of a 'transporting' term proportional to the current strength ($\sim\theta_{\rm str}^{1/2}$ in the case of streaming) and a 'stirring' term ($\sim\theta_{\rm w}^{1/2}\theta_{\rm str}^{1/2}$ by implication).

This method is based upon taking the bed roughness as the sand grain roughness, i.e.

$$z_0 = \frac{2.5d_{50}}{30} \tag{10}$$

in both $\theta_w$ and $\theta_{\rm str}$. However, Nielsen and Callaghan [3] suggested basing the calculation on using Eq. (10) in $\theta_w$, while the bed roughness associated with the bed transport should be used in $\theta_{\rm str}$, i.e. using $z_0 = 170(\theta_w - 0.05)^{1/2}d_{50}/30$. However, the present results will be based on using Eq. (10) in both $\theta_w$ and $\theta_{\rm str}$, as this is considered to be physically more consistent.

The wave mobility number $\Psi$ is defined as

$$\Psi = \frac{U^2}{g(s-1)d_{50}} \tag{11}$$

representing an estimate of the ratio between the disturbing and stabilizing forces acting on a seabed particle [2]. By introducing Eq. (11) Eq. (6) can be re-arranged to

$$\Phi_{\rm str} = \frac{\alpha}{8}kA\left[c\left(\frac{A}{z_0}\right)^{-d}\Psi\right]^{3/2} \tag{12}$$

## 3. Effect of streaming under random waves

### 3.1. General

The present approach is based on the following assumptions:

(1) the free surface elevation $\zeta(t)$ is a stationary Gaussian narrow-band random process with zero expectation described by the single-sided spectral density $S_{\zeta\zeta}(\omega)$,
(2) the bottom friction formula and the bedload transport formula for regular waves given in Section 2, are valid for irregular waves as well.

The second assumption implies that each wave is treated individually and that memory effects are neglected. The validity of this approach was confirmed for seabed shear stresses by Holmedal et al. [19] for high values of $A/z_0$ ($\approx$30000). Characteristic statistical values of the resulting seabed shear stress amplitude deviated less than 20% from those obtained by the Monte Carlo simulation method by Holmedal et al. [18]. Holmedal et al. [18] method is essentially based on the same two assumptions upon which the present approach is based. Regarding the second assumption that each wave is treated individually, Holmedal et al. [19] concluded for large values of $A/z_0$ that the main reason for the fair agreement obtained between the Monte Carlo simulations and the ($k-\varepsilon$) model predictions is the good description of the wave friction factor for individual waves. This appears to be much more important than violating the assumption of independent individual waves. Since the bottom friction formula related to streaming is essentially based on the rough turbulent bed friction factors, the assumption of treating each wave individually for linear waves seems reasonable. Moreover, results from some preliminary studies have been discussed by Myrhaug and Hansen [29]. Overall the results suggested that the present approach is adequate as a first approximation that can be used to predict integrated effects such as bedload sediment transport with a reasonable degree of accuracy. The accuracy of the narrow-band assumption will be discussed below.

Based on the present assumptions, the time-dependent near-bed orbital displacement $a(t)$ and velocity $u(t)$ are both stationary Gaussian narrow-band processes with zero expectations and with single-sided spectral densities as follows:

$$S_{aa}(\omega) = \frac{S_{\zeta\zeta}(\omega)}{\sinh^2 kh} \tag{13}$$

$$S_{uu}(\omega) = \omega^2 S_{aa}(\omega) = \frac{\omega^2 S_{\zeta\zeta}(\omega)}{\sinh^2 kh} \tag{14}$$

For a narrow-band process the waves are specified as a 'harmonic' wave with cyclic frequency $\omega$ and with slowly varying amplitude and phase. Then, for the first order, the near-bed orbital velocity amplitude $U$ is related to the near-bed orbital displacement amplitude $A$ by $U = \omega A$, where $U$ is slowly varying with $t$ as well (see e.g. [30]).

It follows from the narrow-band assumption that the near-bed orbital displacement amplitude, $A$, and the near-bed orbital velocity amplitude, $U$, are Rayleigh-distributed with the cumulative distribution function given as follows:

$$P(\hat{x}) = 1 - \exp(-\hat{x}^2); \quad \hat{x} = x/x_{\mathrm{rms}} \geq 0 \tag{15}$$

where $x$ represents $A$ or $U$, and $x_{\mathrm{rms}}$ is the *rms* value of $x$ representing $A_{\mathrm{rms}}$ or $U_{\mathrm{rms}}$.

Now $A_{\mathrm{rms}}$ and $U_{\mathrm{rms}}$ are related to the zeroth moments of the amplitude and velocity spectra, $m_{0\mathrm{aa}}$ and $m_{0\mathrm{uu}}$, respectively, given as follows:

$$A_{\mathrm{rms}}^2 = 2m_{0aa} = 2\sigma_{aa}^2 = 2\int_0^\infty S_{aa}(\omega)\mathrm{d}\omega \tag{16}$$

$$U_{\mathrm{rms}}^2 = 2m_{0uu} = 2\sigma_{uu}^2 = 2\int_0^\infty S_{uu}(\omega)\mathrm{d}\omega \tag{17}$$

Here $\sigma_{aa}^2$ and $\sigma_{uu}^2$ are the variances of the amplitude and velocity, respectively.

It should be noted that $U_{\mathrm{rms}}$ used by Soulsby [23] corresponds to the standard deviation $\sigma_{\mathrm{uu}}$ used here.

From Eqs. (17) and (14) it also appears that $m_{0uu} = m_{2aa}$, where $m_{2aa} = \int_0^\infty \omega^2 S_{aa}(\omega)\mathrm{d}\omega$ is the second moment of the amplitude spectral density. Thus, the mean zero-crossing frequency for the near-bed orbital displacement, $\omega_z$, is obtained from the spectral moments of $a(t)$ as follows:

$$\omega_z = \left(\frac{m_{2aa}}{m_{0aa}}\right)^{1/2} = \left(\frac{m_{0uu}}{m_{0aa}}\right)^{1/2} = \frac{U_{\mathrm{rms}}}{A_{\mathrm{rms}}} \tag{18}$$

where Eqs. (16) and (17) have been used. This result is valid for a stationary Gaussian random process. Note that for a finite-band process the motion due to higher frequency causes decays more rapidly with depth than lower frequency and therefore contributes less to the motion at the bed. This results in a smaller zero-crossing frequency for $a(t)$ at the bed than at the free surface. However, for a narrow-band process these zero-crossing frequencies will be equal, since there is only one frequency present.

### 3.2. Probability distribution functions

#### 3.2.1. Bottom friction

For a narrow-band process, $A = U/\omega$ where $\omega$ is replaced by $\omega_z$ from Eq. (18) and $A$ is given as follows: $A = UA_{\mathrm{rms}}/U_{\mathrm{rms}}$. Then, by substituting this in Eq. (2) using Eq. (3), Eq. (2) can be re-arranged to give the streaming-related bottom shear stress for the individual narrow-band random wave-cycles as follows:

$$\frac{\tau_{\mathrm{str}}}{\rho} = \frac{\bar{\tau}_{\mathrm{str\ rms}}}{\rho}\left(\frac{U}{U_{\mathrm{rms}}}\right)^{3-d} \tag{19}$$

where, by definition,

$$\frac{\bar{\tau}_{\mathrm{str\ rms}}}{\rho} = \frac{1}{4\sqrt{2}}\bar{k}A_{\mathrm{rms}}U_{\mathrm{rms}}^2 c\left(\frac{A_{\mathrm{rms}}}{z_0}\right)^{-d} \tag{20}$$

and $\bar{k}$ is the wave number corresponding to $\omega_z$ determined from $\omega_z^2 = g\bar{k}\tanh\bar{k}h$. By introducing $\hat{\tau}_{\mathrm{str}} = \tau_{\mathrm{str}}/\bar{\tau}_{\mathrm{str\ rms}}$ and $\hat{U} = U/U_{\mathrm{rms}}$, Eq. (19) can be re-arranged to give the shear stress related to streaming for individual narrow-band random waves as follows:

$$\hat{\tau}_{\mathrm{str}} = \hat{U}^{3-d} \tag{21}$$

Now the cumulative distribution function of $\hat{\tau}_{\mathrm{str}}$ follows by transformation of random variables, when $\hat{U}(\hat{\tau}_{\mathrm{str}})$ same as known. By utilizing $p(\hat{\tau}_{\mathrm{str}}) = p(\hat{U})|d\hat{U}/d\hat{\tau}_{\mathrm{str}}|$ and by using Eq. (15), the cumulative distribution function is given as:

$$P(\hat{\tau}_{\mathrm{str}}) = 1 - \exp(-\hat{\tau}_{\mathrm{str}}^{\beta}); \quad \hat{\tau}_{\mathrm{str}} \geq 0, \quad \beta = \frac{2}{3-d} \tag{22}$$

Hence the distribution of $\hat{\tau}_{\mathrm{str}}$ is given by the Weibull distribution.

When the cumulative distribution function is known, the relevant characteristic statistical values of the bed shear stress caused by streaming under random waves can be calculated. Here only a few characteristic statistical values will be discussed.

The *rms* value is given as follows by using Eq. (22):

$$\hat{\tau}_{\mathrm{str\ rms}} \equiv (E[\hat{\tau}_{\mathrm{str}}^2])^{1/2} = \left[\Gamma\left(1 + \frac{2}{\beta}\right)\right]^{1/2} = [\Gamma(4-d)]^{1/2} \tag{23}$$

The value of $\hat{\tau}_{\mathrm{str}}$ which is exceeded by the probability $1/n$ is given as follows:

$$\hat{\tau}_{\mathrm{str}\ 1/n} = (\ln n)^{1/\beta} = (\ln n)^{(3-d)/2} \tag{24}$$

#### 3.2.2. Bedload transport

By substituting $\omega = \omega_z$ and $A = UA_{\mathrm{rms}}/U_{\mathrm{rms}}$ and using Eqs. (8) and (9), Eq. (6) can be re-arranged to give the bedload transport caused by streaming for individual narrow-band random waves as

$$\Phi_{\mathrm{str}} = \alpha\bar{\theta}_{\mathrm{wrms}}^{1/2}\cdot\theta_{\mathrm{str\ rms}}\left(\frac{U}{U_{\mathrm{rms}}}\right)^{4-\frac{3}{2}d} \tag{25}$$

where, by definition,

$$\bar{\theta}_{\mathrm{wrms}} = \frac{\bar{\tau}_{\mathrm{wrms}}}{\rho g(s-1)d_{50}} \tag{26}$$

$$\frac{\bar{\tau}_{\mathrm{wrms}}}{\rho} = \frac{1}{2}c\left(\frac{A_{\mathrm{rms}}}{z_0}\right)^{-d}U_{\mathrm{rms}}^2 \tag{27}$$

$$\theta_{\mathrm{str\ rms}} = \frac{\bar{\tau}_{\mathrm{str\ rms}}}{\rho g(s-1)d_{50}} \tag{28}$$

and $\bar{\tau}_{\mathrm{str\ rms}}/\rho$ is given in Eq. (20). Eq. (25) can be re-arranged to

$$\phi_{\mathrm{str}} \equiv \frac{\Phi_{\mathrm{str}}}{\alpha\bar{\theta}_{\mathrm{wrms}}^{1/2}\cdot\theta_{\mathrm{str\ \ rms}}} = \hat{U}^{4-\frac{3}{2}d} \tag{29}$$

Now the cumulative distribution function of $\phi_{\mathrm{str}}$ follows by transformation of random variables. Using Eq. (15) with

$\hat{x} = \hat{U}$, gives

$$P(\phi_{\text{str}}) = 1 - \exp(-\phi_{\text{str}}^{\beta}); \quad \phi_{\text{str}} \geq 0, \quad \beta = \frac{2}{4 - \frac{3}{2}d} \tag{30}$$

Hence $\phi_{\text{str}}$ is Weibull distributed.

The statistical value most relevant to the calculation of the bedload sediment transport is the expected (mean) value. The standard deviation is of interest when estimating the spreading of the bedload transport under individual random waves. By using Eq. (30) the expected value and the standard deviation are given as, respectively,

$$E[\phi_{\text{str}}] = \Gamma\left(3 - \frac{3}{4}d\right) \tag{31}$$

$$\sigma(\phi_{\text{str}}) = \left[\Gamma\left(5 - \frac{3}{2}d\right) - \left[\Gamma\left(3 - \frac{3}{4}d\right)\right]^2\right]^{1/2} \tag{32}$$

### 3.3. Friction factor

The friction factors based on characteristic statistical values of the shear stress related to streaming for individual random waves can be defined. The *rms* friction factor is defined as follows:

$$f_{\text{w str,rms}} = \frac{(\tau_{\text{str}}/\rho)_{\text{rms}}}{\frac{1}{2}U_{\text{rms}}^2} \tag{33}$$

Conventional results by using an equivalent sinusoidal wave are obtained by substituting Eq. (3) in (2), and replacing $U$ and $A$ with their *rms*-values, and taking $\omega = \omega_z$ and $k = \bar{k}$ to recover Eq. (20). According to the definition in Eq. (33), the deterministic friction factor is:

$$f_{\text{w str,det}} = \frac{1}{2\sqrt{2}}\bar{k}A_{\text{rms}}c\left(\frac{A_{\text{rms}}}{z_0}\right)^{-d} \tag{34}$$

Similarly, the result according to the present stochastic approach is obtained by substituting $\hat{\tau}_{\text{str rms}} = \tau_{\text{str}}/\bar{\tau}_{\text{str rms}}$ in Eq. (23) using (20). According to the definition in Eq. (33), the stochastic friction factor is:

$$f_{\text{w str,stoch}} = [\Gamma(4-d)]^{1/2} f_{\text{w str,det}} \tag{35}$$

Fig. 2 gives an example of results showing the stochastic and deterministic friction factors divided by $\bar{k}A_{\text{rms}}$ versus $A_{rms}/z_0$. The two lower straight curves represent the stochastic results according to Eq. (35) and the deterministic results according to Eq. (34) for the $(c,d)$ values in Eqs. (4) and (5). Frictions factors based on other characteristic statistical values, e.g. $\hat{\tau}_{\text{str}1/n}$, will have similar behaviour as shown in Fig. 2. The discontinuity in the streaming friction factor is caused by the friction factors for regular waves having different left and right derivatives at the intersection point $A/z_0 = 11000$.

By combining Eqs. (34) and (35), it appears that the stochastic to deterministic method ratio for the *rms* friction factor is given by

$$R_1 = [\Gamma(4-d)]^{1/2} \tag{36}$$

By using the $d$ values in Eqs. (4) and (5), this ratio varies from 1.8 to 2.1 depending on the $A_{rms}/z_0$ range considered. This result is in qualitative agreement with the turbulent boundary layer model results of Deigaard et al. [31]. They used a one-dimensional mixing length model in conjunction with a sediment diffusion model to predict the net sediment

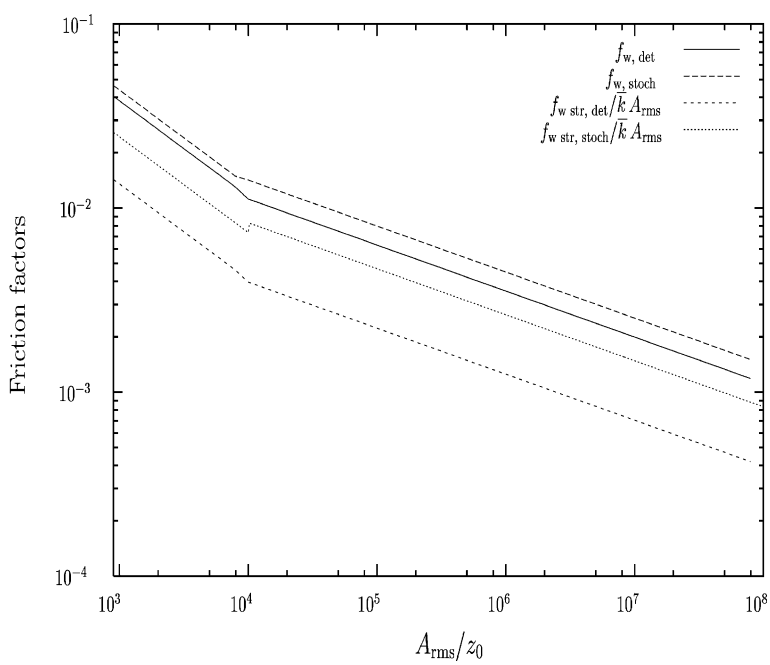


Fig. 2. Friction factors vs. $A_{rms}/z_0$.

Table 1
Bottom friction caused by boundary layer streaming and linear waves

| Flow range | $d$ | Streaming $\hat{\tau}_{\text{str rms}} = [\Gamma(4-d)]^{1/2}$ | $\hat{\tau}_{\text{str }1/n} = (\ln n)^{(3-d)/2}$ | | Linear waves $\hat{\tau}_{\text{rms}} = [\Gamma(3-d)]^{1/2}$ | $\hat{\tau}_{1/n} = (\ln n)^{(2-d)/2}$ | |
|---|---|---|---|---|---|---|---|
| | | | $n=3$ | $n=10$ | | $n=3$ | $n=10$ |
| $900 \lesssim A_{rms}/z_0 \lesssim 11\ 000$ | 0.52 | 1.80 | 1.12 | 2.81 | 1.14 | 1.07 | 1.85 |
| $11\ 000 \lesssim A_{rms}/z_0$ | 0.25 | 2.10 | 1.14 | 3.15 | 1.27 | 1.09 | 2.07 |

transport under wave groups and bound long waves. They found that the shear stress caused by streaming is larger for a wave group than for regular waves with the same energy, i.e. an equivalent sinusoidal wave.

The stochastic results for $\hat{\tau}_{\text{str rms}}$ and $\hat{\tau}_{\text{str }1/n}$ (Eqs. (23) and (24) respectively, using the $d$ values in Eqs. (4) and (5)) are given in Table 1. It should also be noted that $R_1$ (Eq. (36)) coincides with $\hat{\tau}_{\text{str rms}}$ (Table 1) with the present scaling.

### 3.4. Bedload transport

By using Eq. (31) it follows that the expected (mean) value of the dimensionless bedload sediment transport rate due to streaming is given as

$$E[\Phi_{\text{str}}] = \Gamma\left(3 - \frac{3}{4}d\right)\Phi_{\text{str,det}} \tag{37}$$

where $\Phi_{str,\text{det}}$ is the deterministic value obtained by using the equivalent sinusoidal wave concept of replacing the wave-related quantities in Eqs. (6), (8) and (9) with their *rms*-values, giving

$$\Phi_{\text{str,det}} = \alpha\bar{\theta}_{\text{w rms}}^{1/2}\cdot\theta_{\text{str rms}} \tag{38}$$

Here $\bar{\theta}_{\text{w rms}}$ and $\theta_{strrms}$ are as defined in Eqs. (26) and (28), respectively. By using Eqs. (11) and (12), Eq. (38) can be re-arranged to

$$\Phi_{\text{str,det}} = \frac{\alpha}{8}\bar{k}A_{\text{rms}}\left[c\left(\frac{A_{\text{rms}}}{z_0}\right)^{-d}\Psi_{\text{rms}}\right]^{3/2} \tag{39}$$

where

$$\Psi_{\text{rms}} = \frac{U_{\text{rms}}^2}{g(s-1)d_{50}} \tag{40}$$

By using Eq. (32) it follows that the standard deviation of $\Phi_{str}$ is obtained by a similar expression as for $E[\Phi_{str}]$ given in Eq. (37).

From Eq. (37) it follows that the stochastic to deterministic method ratio for the mean bedload transport is given as

$$R_2 = \Gamma\left(3 - \frac{3}{4}d\right) \tag{41}$$

Using the $d$ values in Eqs. (4) and (5), this ratio varies from 1.4 to 1.7 depending on the $A_{rms}/z_0$ range considered. Deigaard et al. [31] also included predictions for bedload transport under wave groups. They found that the bedload transport caused by streaming is slightly larger for a wave group than for regular waves with the same energy, which agrees qualitatively with the present results.

Similarly, the standard deviation can be obtained by using the results in Eq. (32). The standard deviation to mean value ratio, $\sigma(\Phi_{str})/E[\Phi_{str}]$, is given in Table 2, together with the values of $R_2$ for the different roughness regimes. The standard deviation to mean value ratio varies from 1.7 to 2.0 depending on the roughness regime. This shows that $\sigma(\Phi_{str})$ is of the same magnitude as the corresponding $E[\Phi_{str}]$, revealing a significant scatter of the bedload sediment transport rate caused by streaming under random waves.

It should be noted that the expected value of the transport without streaming is zero, i.e. that there are no second order wave asymmetry effects present, consistent with the model assumptions. This wave asymmetry will be addressed in Section 5.

## 4. Bottom friction: Effect of streaming versus effect of linear waves

### 4.1. Bottom friction beneath linear random waves

Here a brief summary of the Myrhaug et al. [14] results for seabed shear stresses under linear random waves is given. They essentially used the same assumptions as in Section 3.1, and found that the non-dimensional maximum bed shear stress for individual random waves was Weibull distributed. This Weibull distribution is given by Eq. (22)

Table 2
Some characteristic statistical values of the bedload sediment transport rate caused by streaming and second order wave asymmetry for the two flow ranges

| Flow range | Stochastic to deterministic method ratio of mean net bedload transport rate $R_2 = \frac{E[\Phi_{\text{str}}]}{\Phi_{\text{str,det}}}, \frac{E[\Phi]}{\Phi_{\text{det}}}$ | Standard deviation to mean value ratio $\frac{\sigma(\Phi_{\text{str}})}{E[\Phi_{\text{str}}]}, \frac{\sigma(\Phi)}{E[\Phi]}$ |
|---|---|---|
| $900 \lesssim A_{rms}/z_0 \lesssim 11\ 000$ | 1.44 | 1.69 |
| $11\ 000 \lesssim A_{rms}/z_0$ | 1.69 | 1.96 |

Table 3
Summary of results for deterministic and stochastic friction factors as well as stochastic to deterministic method ratios for linear waves and that caused by streaming

| | Linear waves | Streaming |
|---|---|---|
| Deterministic method | $f_{w,\det}=c\left(\frac{A_{\mathrm{rms}}}{z_0}\right)^{-d}$ | $f_{\mathrm{w\ str,det}}=\frac{1}{2\sqrt{2}}\bar{k}A_{\mathrm{rms}}c\left(\frac{A_{\mathrm{rms}}}{z_0}\right)^{-d}$ |
| Stochastic method | $f_{w,\mathrm{stoch}}=[\Gamma(3-d)]^{1/2}f_{w,\det}$ | $f_{\mathrm{w\ str,stoch}}=[\Gamma(4-d)]^{1/2}f_{\mathrm{w\ str,det}}$ |
| Stochastic to deterministic method ratio | $R_3=[\Gamma(3-d)]^{1/2}$ | $R_1=[\Gamma(4-d)]^{1/2}$ |

with $\beta=2/(2-d)$; $\hat{\tau}_{\mathrm{str}}$ is replaced by $\hat{\tau}=\tau_w/\bar{\tau}_{\mathrm{w\ rms}}$ where the maximum bed shear stress, $\tau_w$, is made dimensionless by $\bar{\tau}_{\mathrm{w\ rms}}$ given in Eq. (27). Thus, $\hat{\tau}_{\mathrm{rms}}$ and $\hat{\tau}_{1/n}$ are given by similar formulas as in Eqs. (23) and (24), respectively, by using $\beta=2/(2-d)$.

The *rms* friction factor is defined as

$$f_{\mathrm{w,rms}}=\frac{(\tau_w/\rho)_{\mathrm{rms}}}{\frac{1}{2}U_{\mathrm{rms}}^2} \tag{42}$$

By substituting $(\tau_w/\rho)_{\mathrm{rms}}=\hat{\tau}_{\mathrm{rms}}\bar{\tau}_{\mathrm{w\ rms}}/\rho$ in Eq. (42) using Eq. (27) and $\hat{\tau}_{\mathrm{rms}}$ in Table 1, the *rms* friction factor corresponding to the stochastic approach is given in Table 3.

The friction factors $f_{w,stoch}$ and $f_{w,\det}$ are shown in Fig. 2 for the $(c,d)$ values in Eqs. (4) and (5). Friction factors based on other characteristic statistical values, e.g. $\hat{\tau}_{1/n}$, will have similar behaviour as shown in Fig. 2.

The stochastic to deterministic method ratio for the *rms* friction factor, $R_3=f_{w,\mathrm{stoch}}/f_{w,\det}$, is given in Table 3. Using the $d$ values in Eqs. (4) and (5), this ratio varies from 1.1 to 1.3 depending on the $A_{rms}/z_0$ range considered.

The stochastic results for $\hat{\tau}_{\mathrm{rms}}$ and $\hat{\tau}_{1/n}$ using the $d$ values in Eqs. (4) and (5) are given in Table 1. It should be noted that $R_3$ (Table 3) coincides with $\hat{\tau}_{\mathrm{rms}}$ (Table 1) with the present scaling.

### *4.2. Streaming versus linear waves*

Here the effect of streaming versus the effect of linear waves on the bed shear stress will be considered. The shear stress for linear waves in shallow water, for which $\bar{k}h=\pi/10$, will be used as a reference value.

The *rms* value of the shear stress under linear waves is given as

$$\frac{\tau_{\mathrm{wrms}}}{\rho}=\frac{1}{2}c(z_0\omega_z)^d\left(\frac{\omega_z H_{\mathrm{rms}}}{2\sinh\bar{k}h}\right)^{2-d}[\Gamma(3-d)]^{1/2} \tag{43}$$

This result is obtained by combining Eq. (42) with $f_{w,stoch}$ and $f_{w,\det}$ in Table 3 and substitution of $A_{\mathrm{rms}}=U_{\mathrm{rms}}/\omega_z$ and

$$U_{\mathrm{rms}}=\frac{\omega_z H_{\mathrm{rms}}}{2\sinh\bar{k}h} \tag{44}$$

In shallow water, for which $\sinh\bar{k}h\approx\bar{k}h$, Eq. (43) takes the form

$$\frac{\tau_{\mathrm{wrms}}}{\rho}=\frac{1}{2}c(z_0\omega_z)^d\left(\frac{\omega_z H_{\mathrm{rms}}}{2\pi/10}\right)^{2-d}[\Gamma(3-d)]^{1/2} \tag{45}$$

taking $\bar{k}h=\pi/10$.

By combining Eqs. (33) to (35), and substitution of $U_{rms}$ from Eq. (44), the *rms* value of the shear stress caused by streaming is given as

$$\frac{\tau_{\mathrm{str\ \ rms}}}{\rho}=[\Gamma(4-d)]^{1/2}\times\frac{1}{4\sqrt{2}}\bar{k}A_{\mathrm{rms}}c(z_0\omega_z)^d\left(\frac{\omega_z H_{\mathrm{rms}}}{2\sinh\bar{k}h}\right)^{2-d} \tag{46}$$

The range of values of $\bar{k}A_{\mathrm{rms}}$ is determined by the validity of linear wave theory. This can be expressed in terms of the Ursell number requiring $H(2\pi/k)^2/h^3\lesssim 15$ for regular waves [32]. This criterion can be re-arranged to $(kH/2)/(kh)^3\lesssim 0.2$, which for narrow-band random waves is taken as $(\bar{k}H_{\mathrm{rms}}/2)/(\bar{k}h)^3\lesssim 0.2$, where $\bar{k}H_{\mathrm{rms}}/2=\bar{k}A_{\mathrm{rms}}\sinh\bar{k}h$. Thus the Ursell number criterion can be re-arranged to

$$\bar{k}A_{\mathrm{rms}}\lesssim 0.2\frac{(\bar{k}h)^3}{\sinh\bar{k}h} \tag{47}$$

Moreover, the maximum steepness of regular waves in finite water depth is limited by the Miche breaking criterion, i.e. $kH/2\leq\pi\ 0.142\ \tanh(0.875\ kh)$ (see e.g. [23]). For narrow-band random waves this criterion can be re-arranged to

$$\bar{k}A_{\mathrm{rms}}\leq\pi\cdot 0.142\frac{\tanh(0.875\bar{k}h)}{\sinh\bar{k}h} \tag{48}$$

In intermediate water depth ($\pi/10\leq\bar{k}h\leq\pi$) it appears that Eq. (47) is the most restrictive for $\pi/10\leq\bar{k}h\lesssim 1.2$, while Eq. (48) is the most restrictive for $1.2\lesssim\bar{k}h\leq\pi$. Here the shallow to intermediate water depth range $\pi/10\leq\bar{k}h\lesssim 1.2$ is considered, because the seabed shear stress is of most interest in this range. Thus $\bar{k}A_{\mathrm{rms}}$ is restricted by Eq. (47) which for $\bar{k}h=(\pi/10,1.2)$ gives $\bar{k}A_{\mathrm{rms}}\lesssim(0.02,0.23)$. However, since random waves are considered, it can be argued that the criteria in Eqs. (47) and (48) should be based on the maximum wave within the time series, i.e. the maximum values of $H$ and $A$ within the time series should be used rather than the *rms* values. As $H$ and $A$ are Rayleigh-distributed, $(H_{\max},A_{\max})=(H_{\mathrm{rms}},A_{\mathrm{rms}})\sqrt{\ln N}$, where $N$ is the number of waves within the time series. Taking a time series of 1 h duration with a mean zero-crossing wave period of 10 s, $N=360$, giving $(H_{\max},\ A_{\max})\approx 2.4(H_{rms},\ A_{rms})$. In this case the factors used in Eqs. (47) and (48) should be divided by the factor 2.4. Consequently, $\bar{k}A_{\rm rms}$ will be restricted by the modified Eq. (47), which for $\bar{k}h = (\pi/10, 1.2)$ gives $\bar{k}A_{\rm rms} \lesssim (0.01, 0.10)$. Although it is uncertain which values of $H$ and $A$ should be used in the criteria, the present discussion suggests that $\bar{k}A_{\rm rms} = 0.20$ represents an upper limit.

Fig. 3 shows the ratios $R_4$ and $R_5$ versus $\bar{k}h$ in the range $\pi/10$ to 1.2 according to Eqs. (A4) and (A2) (see Appendix A), respectively, for the two flow ranges of $A_{rms}/z_0$. Here $R_4$ is an estimate of the upper limit for the ratio between the shear stress related to streaming (hereafter referred to as the streaming effect) in an arbitrary water depth and the shear stress under linear waves (hereafter referred to as the linear effect) in shallow water. This upper limit is based on the Ursell number criterion in Eq. (47). It appears that $R_4$ is nearly invariant with $\bar{k}h$ for $A_{\rm rms}/z_0 \gtrsim 900$. One should note that the reason for this behaviour of $R_4$ as $\bar{k}h$ increases is caused by the validity range of linear wave theory given by the Ursell number criterion in Eq. (47). $R_5$ is the ratio between the shear stress under linear waves in an arbitrary water depth and in shallow water. In Fig. 3, $R_5$ shows that the linear effect in intermediate water ($\bar{k}h = 1.2$) is an order of magnitude smaller than that in shallow water ($\bar{k}h = \pi/10$). By combining $R_4$ and $R_5$ it appears that the relative magnitude between the streaming effect and the linear effect increases from 1% in shallow water to about 10% in intermediate water. This is also demonstrated in Fig. 4 which shows the ratio between the effect of streaming and the effect of linear waves in an arbitrary water depth ($R_6$) versus $\bar{k}h$.

It should be noted that the results in Figs. 3 and 4 for the *rms* values are similar to those obtained using a deterministic approach. This means that by using a deterministic approach the curves representing $R_4$ and $R_6$ will be reduced by the factor $(3-d)^{1/2}$, while $R_5$ will be the same.

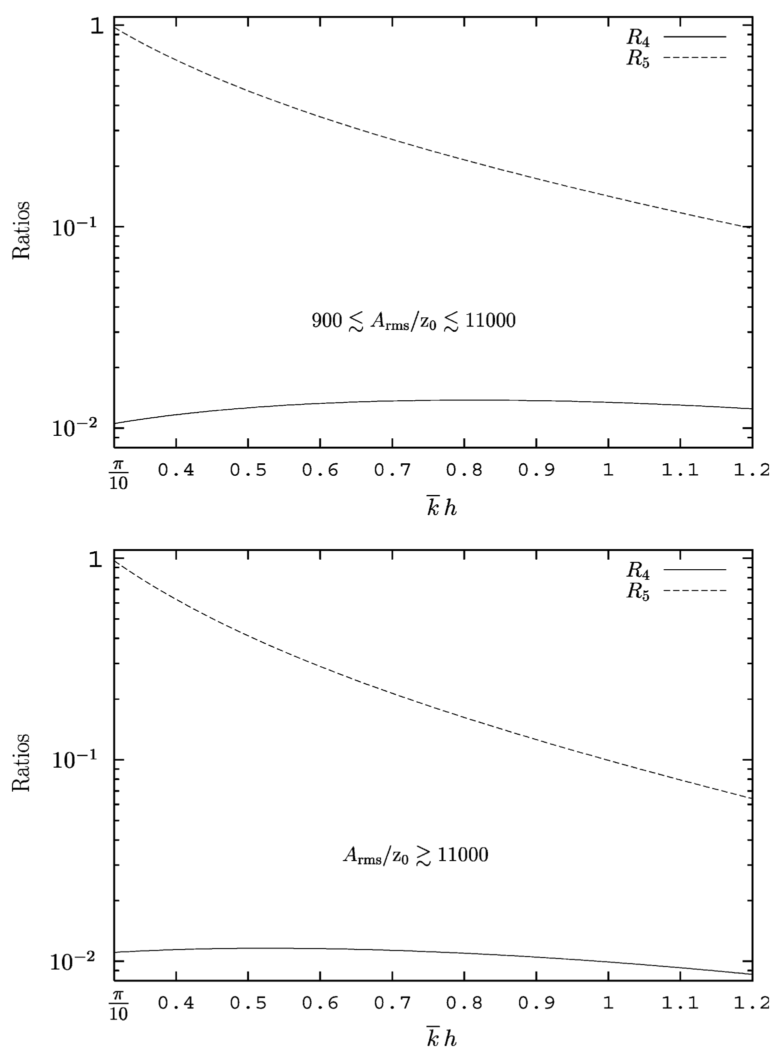


Fig. 3. The ratios $R_4$ (Eq. (A4)), $R_5$ (Eq. (A2)) versus $\bar{k}h$. $R_4$ is an estimate of the upper limit for the ratio between the shear stress caused by streaming in an arbitrary water depth, $\bar{k}h$, and that caused by linear waves in shallow water, $\bar{k}h = \pi/10$. $R_5$ is the ratio between the shear stress under linear waves in an arbitrary water depth and that in shallow water.

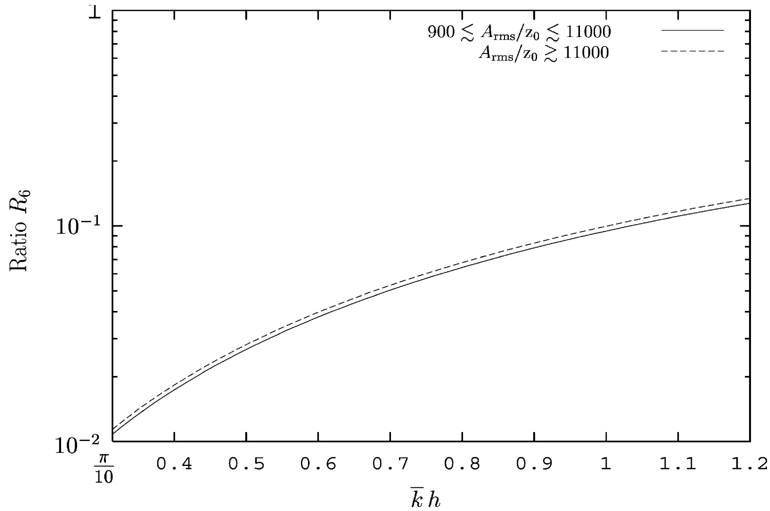


Fig. 4. The ratio $R_6$ (Eq. (A5)) versus $\bar{k}h$. $R_6$ is an estimate of the upper limit for the ratio between the shear stress caused by streaming and that caused by linear waves in an arbitrary water depth, $\bar{k}h$.

## 5. Bedload transport: Effect of streaming versus effect of Stokes second order wave asymmetry

### 5.1. Bedload transport by nonlinear random waves

Here a brief summary of the [9] results for the bedload sediment transport rate by nonlinear random waves is given. They essentially used the same assumptions as in Section 3.1 except for using the [25] bedload transport formula for second order regular waves, which was assumed to be valid for second order nonlinear irregular waves as well. The cumulative distribution function of the nondimensional net bedload sediment transport rate for individual narrow-band random waves was found to be Weibull distributed, i.e. given by Eq. (30) with $\phi_{str}$ replaced by $\phi$. Here

$$\phi = \frac{\Phi}{2.8\Delta_{\rm rms}\bar{\theta}_{\rm w\ rms}^{3/2}} \tag{49}$$

$$\Phi = \frac{q_b}{[g(s-1)d_{50}^3]^{1/2}} \tag{50}$$

where $\Delta_{rms}$ and $\bar{\theta}_{\rm w\ rms}$ are given in Table 4 and Eq. (26), respectively, and $q_b$ is the volumetric net bedload transport rate per unit width [$m^2/s$]. Thus the expected value, $E[\phi]$, and the standard deviation, $\sigma[\phi]$, are as given in Eqs. (31) and (32), respectively.

Here $0 \le \Delta_{\rm rms} \lesssim 0.20$ represents a characteristic asymmetry of the shear stress (caused by second order wave asymmetry) in a seastate of random waves. The range of $\Delta_{rms}$ values follows by substituting the upper limit of $\bar{k}A_{\rm rms}$ from Eq. (47) in $\Delta_{rms}$ given in Table 4, which for $\bar{k}h = (\pi/10, 1.2)$ gives $\Delta_{\rm rms} \lesssim (0.2, 0.1)$. However, if the criterion in Eq. (47) is based on the maximum wave in a time series of 1 h duration, then these values of $\Delta_{rms}$ should be divided by the factor 2.4 as explained in Section 4.2. Due to the uncertainty related to which values of $A$ to use in the criterion in Eq. (47), it is suggested that $\Delta_{rms} = 0.2$ represents an upper limit.

By using Eqs. (49) and (31) with $\phi_{str}$ replaced by $\phi$ it follows that $E[\Phi]$ and $\Phi_{\rm det}$ are as given in Table 4.

By using the results in Table 4 it follows that the stochastic to deterministic method ratio for the mean bedload transport rate is given by $R_2$ in Eq. (41). Similarly, the standard deviation can be obtained by using the result in Eq. (32). The standard deviation to mean value ratio, $\sigma(\Phi)/E[\Phi]$, is given in Table 2, together with the values of $R_2$ for the different roughness regimes. Moreover, a significant scatter of the bedload sediment transport caused by second

Table 4
Summary of results for deterministic and stochastic method results for mean bedload transport rate caused by streaming and second order wave asymmetry

| | Streaming | Second order wave asymmetry |
|---|---|---|
| Deterministic method | $\Phi_{\rm str,det} = \alpha\bar{\theta}_{w\rm rms}^{1/2}\cdot\theta_{\rm str\quad rms} = \frac{\alpha}{8}\bar{k}A_{\rm rms}\left[c\left(\frac{A_{\rm rms}}{z_0}\right)^{-d}\Psi_{\rm rms}\right]^{3/2}$ | $\Phi_{\rm det} = 2.8\Delta_{\rm rms}\bar{\theta}_{w\rm rms}^{3/2} = 2.8\left[2-\left(1-\frac{2}{\pi}\right)d\right]\frac{3}{8\sqrt{2}} \times\frac{\bar{k}A_{\rm rms}}{\sinh^2\bar{k}h}\left[c\left(\frac{A_{\rm rms}}{z_0}\right)^{-d}\Psi_{\rm rms}\right]^{3/2}$ |
| Stochastic method | $E[\Phi_{\rm str}] = \Gamma\left(3-\frac{3}{4}d\right)\Phi_{\rm str,det}$ | $E[\Phi] = \Gamma\left(3-\frac{3}{4}d\right)\Phi_{\rm det}$ |
| Stochastic to deterministic method ratio | $R_2 = \Gamma\left(3-\frac{3}{4}d\right)$ | $R_2 = \Gamma\left(3-\frac{3}{4}d\right)$ |

$\Delta_{\rm rms} = \left[2-\left(1-\frac{2}{\pi}\right)d\right]\frac{3\bar{k}H_{\rm rms}}{8\sinh^3\bar{k}h} = \left[2-\left(1-\frac{2}{\pi}\right)d\right]\frac{3\bar{k}A_{\rm rms}}{8\sinh^2\bar{k}h}$ = characteristic asymmetry; $H_{\rm rms} = \left[8\int_0^\infty S_{\zeta\zeta}(\omega)\mathrm{d}\omega\right]^{1/2}$ = *rms* value of wave height.

order wave asymmetry was revealed. A similar scatter was found in field data of ripple migration rates (related to bedload) by Amos et al. [33]. Such a scatter was also estimated by Holmedal and Myrhaug [24].

### 5.2. Streaming versus second order wave asymmetry

Here the relative magnitude of the mean bedload transport caused by random second order Stokes wave asymmetry and the mean bedload transport caused by streaming for random waves will be considered. The mean bedload transport caused by streaming in shallow water, for which $\bar{k}h=\pi/10$, will be used as a reference.

By combining Eqs. (29) and (31), and substitution of $U_{rms}$ from Eq. (44), the mean bedload transport caused by streaming is given as

$$E[\Phi_{\rm str}] = \Gamma\left(3-\frac{3}{4}d\right)\frac{\alpha[c(\omega_z z_0)^d]^{3/2}\bar{k}A_{\rm rms}\left[\frac{\omega_z H_{\rm rms}}{2\sinh \bar{k}h}\right]^{3-\frac{3}{2}d}}{8[g(s-1)d_{50}]^{3/2}} \tag{51}$$

An estimate of the upper limit of $E[\Phi_{str}]$ for $\bar{k}h$ in the range $\pi/10$ to 1.2 is obtained by substituting the upper limit of $\bar{k}A_{\rm rms}$ given by the Ursell number criterion, Eq. (47), in Eq. (51), which gives

$$E[\Phi_{\rm str}] = \Gamma\left(3-\frac{3}{4}d\right)\frac{\alpha[c(\omega_z z_0)^d]^{3/2}0.2\frac{(\bar{k}h)^3}{\sinh \bar{k}h}\left[\frac{\omega_z H_{\rm rms}}{2\sinh \bar{k}h}\right]^{3-\frac{3}{2}d}}{8[g(s-1)d_{50}]^{3/2}} \tag{52}$$

By using the results in Table 4 and substitution of $U_{rms}$ from Eq. (44), the mean bedload transport caused by second order wave asymmetry is given as

$$E[\Phi] = \Gamma\left(3-\frac{3}{4}d\right)\cdot 2.8\left[2-\left(1-\frac{2}{\pi}\right)d\right] \cdot\frac{3\bar{k}A_{\rm rms}}{8\sqrt{2}\sinh^2 \bar{k}h}\frac{[c(\omega_z z_0)^d]^{3/2}\left[\frac{\omega_z H_{\rm rms}}{2\sinh \bar{k}h}\right]^{3-\frac{3}{2}d}}{[g(s-1)d_{50}]^{3/2}} \tag{53}$$

It should be noted that the bedload process that contribute to Eq. (53) is as follows: It represents no more than the transport arising from the enhanced stresses beneath the wave crests compared with the smaller stresses beneath the wave troughs.

An estimate of the upper limit of $E[\Phi]$for $\bar{k}h$ in the range $\pi/10$ to 1.2 is obtained by substituting the upper limit of $\bar{k}A_{\rm rms}$ from Eq. (47) in (53), which gives

$$E[\Phi] = \Gamma\left(3-\frac{3}{4}d\right)\cdot 2.8\left[2-\left(1-\frac{2}{\pi}\right)d\right] \cdot\frac{0.6(\bar{k}h)^3}{8\sqrt{2}\sinh^3 \bar{k}h}\frac{[c(\omega_z z_0)^d]^{3/2}\left[\frac{\omega_z H_{\rm rms}}{2\sinh \bar{k}h}\right]^{3-\frac{3}{2}d}}{[g(s-1)d_{50}]^{3/2}} \tag{54}$$

Fig. 5 shows the ratios $R_7$ and $R_8$ versus $\bar{k}h$ in the range $\pi/10$ to 1.2 according to Eqs. (B1) and (B2) (see Appendix B), respectively, for the two flow ranges of $A_{rms}/z_0$. It appears that the ratio between the mean bedload transport caused by streaming in an arbitrary water depth and that in shallow water (based on an estimate of the upper limit of $E[\Phi_{str}]$) ($R_7$) is reduced by a factor between 3 and 5 from shallow to intermediate water for $A_{\rm rms}/z_0 \gtrsim 900$ depending on the $A_{rms}/z_0$ range. Moreover, the ratio between the mean bedload transport caused by second order wave asymmetry in an arbitrary water depth and the mean bedload transport caused by streaming in shallow water (based on upper limits of both effects) ($R_8$) is reduced by two orders of magnitude from shallow to intermediate water for $A_{\rm rms}/z_0 \gtrsim 900$. Overall it also appears that the second order wave asymmetry effect is nearly an order of magnitude larger than the streaming effect in shallow water, while the two effects are approximately of the same order of magnitude in intermediate water. This is also demonstrated in Fig. 6 showing the ratio between the effect of second order wave asymmetry and the effect of streaming in an arbitrary water depth ($R_9$) versus $\bar{k}h$. Thus the results in Figs. 5 and 6 imply that the total mean bedload transport caused by second order wave asymmetry and streaming in intermediate water is reduced to between 3% to 6% of the total bedload transport in shallow water for $A_{\rm rms}/z_0 \gtrsim 900$ depending in the $A_{rms}/z_0$ range.

It should be noted that the results in Figs. 5 and 6 are the same as those obtained using a deterministic approach, that is, by using the equivalent sinusoidal wave representation the curves representing the ratios $R_7$, $R_8$ and $R_9$ will be the same.

## 6. Stochastic versus deterministic approach

It has been shown that the present stochastic approach for the prediction of both bed friction and bedload transport gives larger values than the deterministic prediction based on an equivalent sinusoidal wave. For the effects caused by streaming these results are in qualitative agreement with the modelling results of Deigaard et al. [31]. Holmedal et al. [19] found good agreement between the prediction of bed friction under random waves plus current by a $(k-\varepsilon)$ model and the [18] prediction using a Monte Carlo simulation based on parameterized friction factor formulas for sinusoidal waves plus current. This supports the present stochastic approach for bed friction, as Holmedal et al. [18] essentially used the same assumptions as in Section 3.1. However, it should be recalled that the present method is based on idealized conditions and, as such, the results should be taken as a first approximation. Confidence in the results can only be supported by measurements or simulations for random waves. However, to separate the streaming effects in experiments are both difficult and challenging; two-dimensional simulations for random waves are also demanding. In the meantime the present

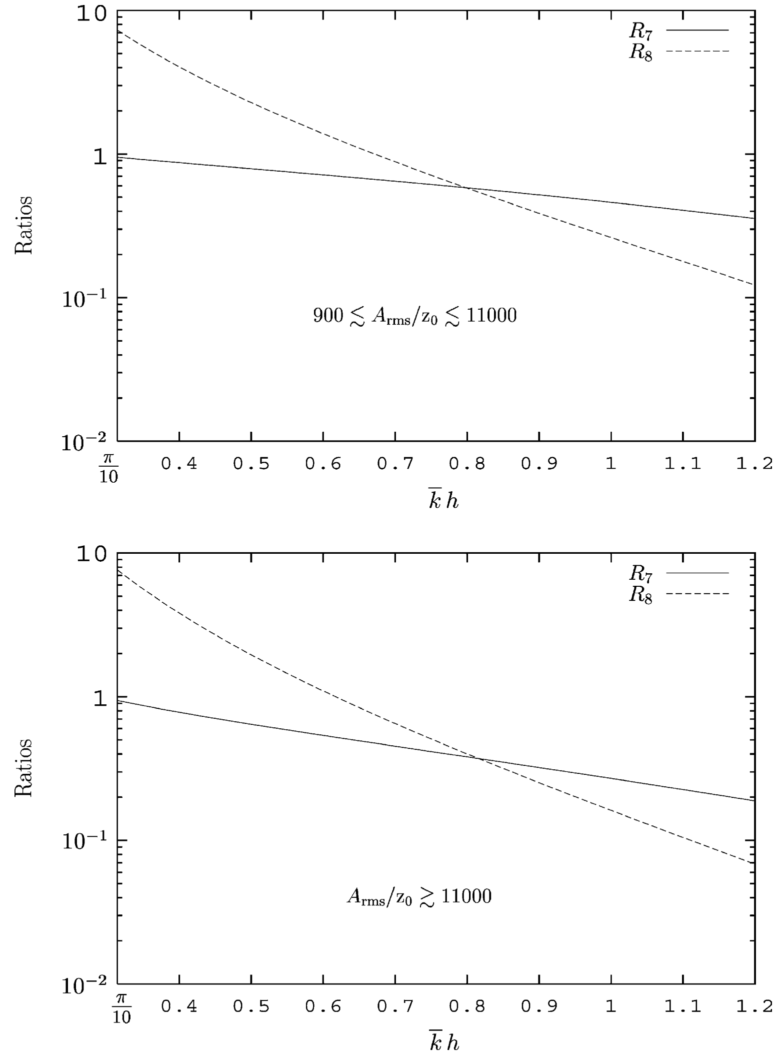


Fig. 5. The ratios $R_7$ (Eq. (B1)) and $R_8$ (Eq. (B2)) versus $\bar{k}h$. $R_7$ is an estimate of the upper limit for the ratio between the mean bedload transport rate caused by streaming in an arbitrary water depth, $\bar{k}h$, and that in shallow water, $\bar{k}h = \pi/10$. $R_8$ is an estimate of the upper limit for the ratio between the mean bedload transport rate caused by second order wave asymmetry in an arbitrary water depth and that caused by streaming in shallow water.

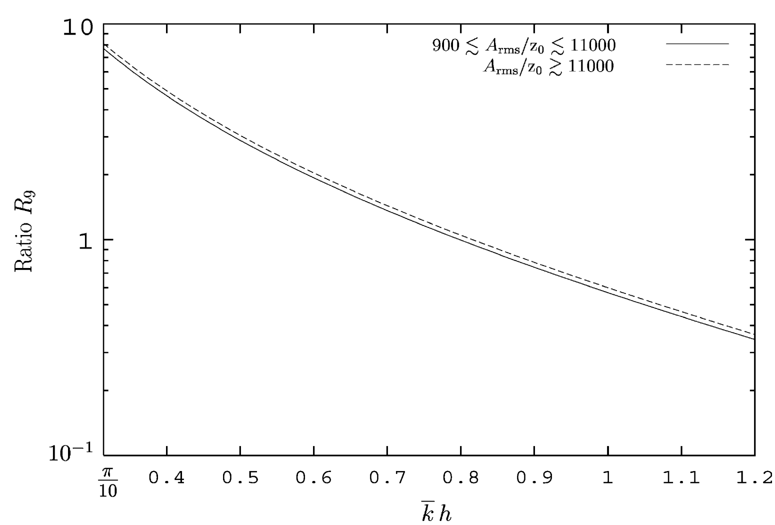


Fig. 6. The ratio $R_9$ (Eq. (B3)) versus $\bar{k}h$. $R_9$ is the ratio between the mean bedload transport rate caused by second order wave asymmetry and that caused by streaming in an arbitrary water depth, $\bar{k}h$.

approach should serve as a useful tool for estimating the effect of streaming on bed friction and bedload transport under random waves.

## 7. Summary and conclusions

An approach is presented by which the effects of boundary layer streaming on the seabed shear stresses, and the mean bedload transport rate, beneath random waves are investigated. It is demonstrated how bottom friction formulas and bedload transport rate formulas for regular waves can be used to obtain the bed shear stresses and the mean bedload transport rate resulting from steady streaming under random waves. As a result, friction factors for steady streaming under random waves are provided, and the effect of streaming versus the effect of linear waves is discussed. Moreover, for the mean bedload transport rate the effect of boundary layer streaming versus the effect of second order wave asymmetry is discussed. The results are valid for flat rough beds with $A/z_0 \gtrsim 900$, for which the streaming is in the direction of wave propagation. The bedload transport caused by second order wave asymmetry is also in the wave propagation direction. The present analysis of bed shear stresses has physical implications for the estimation of wave energy dissipation for flow above rough beds. The results for the mean bedload transport rate are particularly relevant to shingle and coarse sand, where all, or at least most, of the sediment transport takes place as bedload.

For bottom friction the main conclusions are:

(a) The present stochastic approach gives 1.4–2.1 larger friction factors related to streaming than those obtained using *rms* values in an otherwise deterministic approach.
(b) The typical values exemplified for shallow ($\bar{k}h = \pi/10$) to intermediate ($\bar{k}h = 1.2$) water depths based on upper estimates of the *rms* values of the seabed shear stresses caused by streaming, suggest that:

The relative magnitude between the streaming effect and the linear effect increases from 1% in shallow water to about 10% in intermediate water. This is because the streaming effect in intermediate water is about the same as in shallow water; this is a consequence of the upper validity range of linear wave theory given by the Ursell number criterion. Consequently, the sum of the linear and streaming effects in intermediate water is about 10% of the linear effect in shallow water.

For bedload transport rate the main conclusions are:

(a) The present stochastic approach gives 1.4 to 1.7 larger mean bedload transport rate caused by streaming than those obtained by using *rms* values in an otherwise deterministic approach.
(b) The standard deviation of the bedload transport caused by streaming is of the same magnitude as the mean bedload transport, revealing a significant scatter of the bedload transport caused by streaming.
(c) The same conclusions as given in (a) and (b) are also valid for the bedload transport rate caused by second order wave asymmetry.
(d) The typical values exemplified for shallow ($\bar{k}h = \pi/10$) to intermediate ($\bar{k}h = 1.2$) water depths based on upper estimates of the mean bedload transport rates caused by streaming and second order wave asymmetry, suggest that:

- Overall the effect of second order wave asymmetry is nearly an order of magnitude larger than the streaming effect in shallow water; the two effects are of the same order of magnitude in intermediate water.
- The total mean bedload transport rate caused by streaming and second order wave asymmetry in intermediate water is reduced to about 5% of the total bedload transport rate in shallow water.

Overall, the present results for the prediction of both bed friction and bedload transport give larger values than the deterministic prediction based on an equivalent sinusoidal wave. For the effects caused by streaming these results are in qualitative agreement with the modelling results of Deigaard et al. [31].

## Acknowledgements

This work was carried out as part of the SANDPIT project ‘Sand Transport and Morphology of Offshore Sand Mining Pits/Areas’, funded by the European Commission Research Directorate-General Contract No. EVK3-CT-2001-00056/SANDPIT.

## Appendix A. Ratios for bed shear stress caused by streaming and linear waves

A measure of the relative magnitude between the effects of streaming in an arbitrary water depth and linear waves in shallow water, $R_4$, is obtained by taking the ratio of Eqs. (46) and (45), which gives

$$R_{4*} = \frac{(3-d)^{1/2}}{2\sqrt{2}} \bar{k} A_{\mathrm{rms}} \left( \frac{\pi/10}{\sinh \bar{k}h} \right)^{2-d} \tag{A1}$$

The ratio between the shear stress under linear waves in arbitrary water depth and in shallow water, $R_5$, is obtained by taking the ratio of Eqs. (43) and (45), which gives

$$R_5 = \left( \frac{\pi/10}{\sinh \bar{k}h} \right)^{2-d} \tag{A2}$$

Moreover, the ratio between the effect of streaming and the effect of linear waves in an arbitrary water depth, $R_{6*}$, is obtained by taking the ratio of Eqs. (46) and (43), giving

$$R_{6*} = \frac{(3-d)^{1/2}}{2\sqrt{2}}\bar{k}A_{\mathrm{rms}} \tag{A3}$$

An estimate of the upper limit of the relative magnitude between the effects of streaming in an arbitrary water depth (for $\pi/10 \le \bar{k}h \le 1.2$) and linear waves in shallow water, $R_4$, can be obtained by substituting the upper limit of $\bar{k}A_{\mathrm{rms}}$ from Eq. (47)(the Ursell number criterion) in Eq. (A1), which gives

$$R_4 = \frac{(3-d)^{1/2}}{2\sqrt{2}} \cdot 0.2\frac{(\bar{k}h)^3}{\sinh \bar{k}h} \cdot \left(\frac{\pi/10}{\sinh \bar{k}h}\right)^{2-d} \tag{A4}$$

Moreover, an estimate of the upper limit for the ratio between the effect of streaming and the effect of linear waves in an arbitrary water depth (for $\pi/10 \le \bar{k}h \le 1.2$), $R_6$, is obtained by substitution of the upper limit of $\bar{k}A_{\mathrm{rms}}$ from Eq. (47) in Eq. (A3) (or by taking the ratio of Eqs. (A4) and (A2)), which gives

$$R_6 = \frac{(3-d)^{1/2}}{2\sqrt{2}}0.2\frac{(\bar{k}h)^3}{\sinh \bar{k}h} \tag{A5}$$

## Appendix B. Ratios for mean bedload transport caused by streaming and second order wave asymmetry

The shallow water value of the mean bedload transport caused by streaming for $\bar{k}h = \pi/10$ is obtained from Eq. (52) by substituting $\sinh \bar{k}h = \bar{k}h = \pi/10$. Thus the ratio between the mean bedload transport caused by streaming in an arbitrary water depth and in shallow water ($\bar{k}h = \pi/10$) is obtained as (based on an estimate of the upper limit of $E[\Phi_{str}]$)

$$R_7 = (\pi/10)^{1-\frac{3}{2}d}\frac{(\bar{k}h)^3}{(\sinh \bar{k}h)^{4-\frac{3}{2}d}} \tag{B1}$$

A measure of the relative magnitude between the effect of second order wave asymmetry in an arbitrary water depth and the effect of streaming in shallow water (based on upper limits of both effects) is obtained by taking the ratio of Eqs. (54) and (52) (for $\sinh \bar{k}h = \bar{k}h = \pi/10$ in Eq. (52)),

$$R_8 = \frac{2.8}{\alpha}\left[2-\left(1-\frac{2}{\pi}\right)d\right]\frac{3}{\sqrt{2}}\left(\frac{\pi}{10}\right)^{1-\frac{3}{2}d}\frac{(\bar{k}h)^3}{(\sinh \bar{k}h)^{6-\frac{3}{2}d}} \tag{B2}$$

Moreover, the ratio between the effect of second order wave asymmetry and the effect of streaming in an arbitrary water depth (for $\pi/10 \le \bar{k}h \le 1.2$) is obtained by taking the ratio of $\Phi_{\mathrm{det}}$ and $\Phi_{str,\mathrm{det}}$ in Table 4, giving

$$R_9 = \frac{2.8}{\alpha}\left[2-\left(1-\frac{2}{\pi}\right)d\right]\frac{3}{\sqrt{2}}\frac{1}{\sinh^2 \bar{k}h} \tag{B3}$$

## References

[1] Longuet-Higgins MS. The mechanics of the boundary layer near the bottom in a progressive wave. Proc. 6th Int. Conf. Coastal Eng., ASCE, Miami 1956;184–93.
[2] Nielsen P. Coastal Bottom Boundary Layers and Sediment Transport. Singapore: World Scientific Publishing; 1992.
[3] Nielsen P, Callaghan DP. Shear stress and sediment transport calculations for sheet flow under waves. Coastal Eng 2003;47:347–54.
[4] Ribberink JS, Dohmen-Janssen CM, Hanes DM, McLean SR, Vincent C. Near-bed sand transport mechanisms under waves. Proceedings of 27th International Conference on Coastal Engineering, ASCE, Sydney, Australia 2000.
[5] Davies AG, Villaret C. Oscillatory flow over rippled beds: Boundary layer structure and wave-induced Eulerian drift. In: Hunt JN, editor. Gravity Waves in Water of Finite Depth. Advances in Fluid Mechanics, 1997. p. 215–54. Chapter 6.
[6] Davies AG, Villaret C. Wave-induced currents above rippled beds. In: Dronkers J, Scheffers M, editors. Physics of Estuaries and Coastal Seas. Rotterdam: A.A. Balkema; 1998.
[7] Davies AG, Villaret C. Eulerian drift induced by progressive waves above rippled and very rough beds. J Geophys Res 1999;104(C1): 1465–88.
[8] Trowbridge J, Madsen OS. Turbulent wave boundary layers. 2. Second-order theory and mass transport. J Geophys Res 1984;89(C5): 7999–8007.
[9] Myrhaug D, Holmedal LE. Bedload sediment transport rate by nonlinear random waves. Coastal Eng J 2001;43:133–42.
[10] Madsen OS. Spectral wave-current bottom boundary layer flows. Proc. 24th Int. Conf. Coastal Eng., ASCE, Kobe, Japan 1994;384–98.
[11] Simons RR, Grass TJ, Tehrani MM. Bottom shear stresses under random waves with a current superimposed. Proceedings of 24th International Conference on Coastal Engineering, Kobe, Japan, ASCE 1994;565–78.
[12] Simons RR, MacIver RD, Saleh WM. Kinematics and shear stresses from combined waves and longshore currents in the UK coastal research facility. Proc. 25th Int. Conf. Coastal Eng., ASCE, Orlando 1996.
[13] Myrhaug D. Bottom friction beneath random waves. Coastal Eng 1995;24:259–73.
[14] Myrhaug D, Holmedal LE, Simons RR, MacIver RD. Bottom friction in random waves plus current flow. Coastal Eng 2001;43:75–92.
[15] Myrhaug D, Slaattelid OH, Lambrakos KF. Seabed shear stresses under random waves: Predictions versus estimates from field measurements. Ocean Eng 1998;25:907–16.
[16] Mathiesen PP, Madsen OS. Waves and currents over a fixed rippled bed 3. Bottom and apparent roughness for spectral waves and currents. J Geophys Res 1999;104(C8):18447–61.
[17] M.A. Samad, Investigation of bottom boundary layer under irregular waves, PhD thesis, Department of Civil Engineering, Tohoku University, Aoba, Sendai, Japan, 2000.
[18] Holmedal LE, Myrhaug D, Rue H. Seabed shear stresses under irregular waves plus current from Monte Carlo simulations of parameterized models. Coastal Eng 2000;39:123–47.
[19] Holmedal LE, Myrhaug D, Rue H. The sea bed boundary layer under random waves plus current. Continental Shelf Res 2003;23:717–50 err. 1035.

[20] Myrhaug D, Holmedal LE. Bottom friction in nonlinear random waves plus current flow. Proc. 28th Int. Conf. Coastal Eng., ASCE, Cardiff, Wales 2002;1:545–56.

[21] Myrhaug D, Holmedal LE. Laminar bottom friction beneath nonlinear random waves. Coastal Eng J 2003;45:49–61.

[22] Myrhaug D, Holmedal LE. Bottom friction caused by boundary layer streaming beneath random waves for laminar and smooth turbulent flow. Ocean Eng 2005;32:195–222.

[23] Soulsby RL. Dynamics of Marine Sands. London, UK: Thomas Telford; 1997.

[24] Holmedal LE, Myrhaug D. Bed load transport under irregular waves plus current from Monte Carlo simulations of parameterized models with application to ripple migration rates observed in the field. Coastal Eng 2004;51:155–72.

[25] Damgaard JS, Stripling S, Soulsby RL. Numerical modeling of coastal shingle transport, Report TR4. Wallingford, UK: HR Wallingford; 1996.

[26] Schlichting H. Boundary-Layer Theory. 7th ed. New York: McGraw-Hill; 1979.

[27] Swart DH. Offshore sediment transport and equilibrium beach profiles. Publ.131 Delft Hydraulics Lab. The Netherlands: Delft; 1974.

[28] Justesen, P. (1988). Turbulent wave boundary layers. Series Paper 43. PhD thesis, Techn. Univ. Denmark, Inst. of Hydrodynamics and Hydraulic Engineering, ISVA, Lyngby, Denmark.

[29] Myrhaug D, Hansen EH. Long-term distribution of seabed shear stresses beneath random waves. Coastal Eng 1997;31:327–37.

[30] Sveshnikov AA. Applied Methods in the Theory of Random Functions. New York: Pergamon Press; 1966.

[31] Deigaard R, Jakobsen JB, Fredsøe J. Net sediment transport under wave groups and bound long waves. J Geophys Res 1999;104(C6): 13559–75.

[32] Skovgaard O, Svendsen IA, Jonsson IG, Brink-Kjær O. Sinusoidal and cnoidal gravity waves formulae and tables. Institute of Hydrodynamics and Hydraulic Engineering (ISVA), Lyngby. Denmark: Technical University of Denmark; 1974.

[33] Amos CL, Bowen AJ, Huntley DA, Judge J, Li MZ. Ripple migration and sand transport under quasi-orthogonal combined flows on the Scotian Shelf. J. Coastal Res. 1999;15(1):1–15.